Journal of Materials Science: Materials in Medicine (2025)36:6
https://doi.org/10.1007/s10856-024-06856-1

BIOMATERIALS SYNTHESIS AND CHARACTERIZATION

Review Article

Understanding the relationship between pore structure and properties of triply periodic minimal surface bone scaffolds

Yadi Sun[1,2,3,4] · Yan Wang[1,2,3] · Benchao Dong[1,2,3] · Peichuan Yang[1,2,3] · Chunhui Ji[5] · Yiyang Li[1,2,3] · Jianxiong Ma[1,2,3] · Xinlong Ma[1,2,3]

Received: 5 September 2024 / Accepted: 18 December 2024

Abstract

The number of patients with bone defects caused by trauma and diseases has been increasing year by year. The treatment of bone defects remains a major challenge in clinical practice. Bone scaffolds are increasingly favored for repairing bones, with triply periodic minimal surface (TPMS) scaffolds emerging as a popular option due to their superior performance. The aim of this review is to highlight the crucial influence of pore structure on the properties of TPMS bone scaffolds, offering important insights for their innovation and production. It briefly examines various elements that influence the properties of TPMS bone scaffolds, such as pore shape, porosity, pore diameter, and curvature. By analyzing these elements, this review serves as a valuable reference for upcoming research and practical implementations in the field of bone tissue engineering.

Graphical Abstract

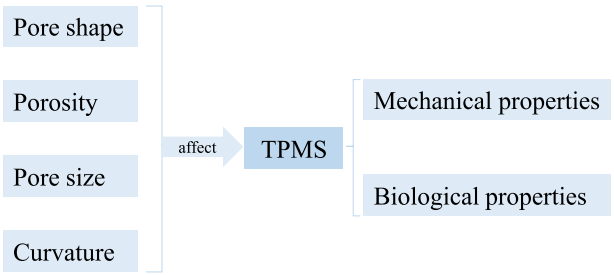

1 Introduction

Bone defects resulting from trauma and various other factors are frequently encountered in clinical settings, with more than 20 million individuals affected globally each year [1, 2]. Such defects can lead to significant pain, restrict physical function, and greatly diminish the quality of life for patients. It is crucial to expedite the repair of these defects and enhance the efficacy of the healing process, as these are pressing challenges that require attention [3]. While autologous bone grafting is recognized as the "gold standard" for treating bone deficiencies and has proven effective in restoring bone function, it carries substantial surgical risks and has limitations in its clinical use [4]; similarly, the use of allogeneic bone grafts is constrained by potential immune reactions [1]. Bone scaffolds, offering an unrestricted alternative, are vital in the clinical management of

These authors contributed equally: Yadi Sun, Yan Wang

✉ Jianxiong Ma
yjslwtg@126.com

[1] Tianjin Hospital Tianjin University, Tianjin, China

[2] Tianjin Orthopedic Institute, Tianjin, China

[3] Tianjin Key Laboratory of Orthopedic Biomechanics and Medical Engineering, Tianjin, China

[4] Academy of Medical Engineering and Translational Medicine, Tianjin University, Tianjin, China

[5] School of Mechanical Engineering, Tianjin University, Tianjin, China

Published online: 07 January 2025

bone defects, as they provide both mechanical support and the essential conditions for bone tissue formation [5].

In bone tissue engineering, having a well-structured internal architecture is crucial for scaffolds, and the design of these scaffolds is of great significance [6]. Recent developments in additive manufacturing and computer-aided design have enabled the production of intricate and easily modifiable porous scaffolds [7]. Recently, triply periodic minimal surfaces (TPMS) structures have become increasingly popular in bone implant applications, especially in the design of bone scaffolds, due to their similarities to bone structure [8, 9]. TPMS, with its continuity and periodicity, exhibits non-self-intersecting surface characteristics in three-dimensional space and has a constant average curvature of zero [10, 11]. This zero curvature property makes TPMS smooth in internal topology. Compared with simple geometric shapes with straight edges or sharp corners, TPMS is more conducive to stress transmission and can achieve more uniform stress distribution, thereby effectively reducing stress concentration [12, 13]. Since TPMS is defined by implicit equations, it can change properties such as pore size and porosity by adjusting parameters, which is crucial to meet the different requirements of structural parameters in different parts [14, 15]. This parameter adjustment capability makes the internal structure of TPMS closer to natural bone, thereby providing good mechanical properties and bioadaptability, creating suitable conditions for bone tissue growth [16, 17].

Given that the internal porosity significantly influences scaffold performance, it is essential to thoughtfully design porous materials to satisfy the mechanical, mass transfer, and biological needs of specific applications. This article examines the advancements in TPMS bone scaffolds, analyzes the effects of their pore architecture on functionality, elucidates the mechanisms through which the pore structure of TPMS bone scaffolds influences performance, and offers insights for the design of bone scaffolds.

2 Introduction to TPMS

TPMS is a type of structure that exists in nature. Triple periodic minimal surfaces have been found in organisms such as sea urchins, biofilms, butterfly wing scales, and beetle exoskeletons [18]. Minimal surfaces are surfaces whose mean curvature is 0 everywhere, that is, they satisfy $H = (k_1 + k_2)/2 = 0$, where k_1 and k_2 are the principal curvatures [19]. When a minimal surface is periodically arranged in three independent directions, the corresponding surface is called a triple periodic minimal surface. The structure of TPMS is a topological structure that can be controlled by mathematical functions. The common expression is [20]:

$$\mathrm{P}: \quad \Phi P(x,y,z) = \cos\omega x + \cos\omega y + \cos\omega z = c \tag{1}$$

$$\mathrm{G}: \quad \Phi G(x,y,z) = \sin\omega x\cos\omega y + \sin\omega\omega x\cos z + \sin\omega x\cos\omega x = c \tag{2}$$

$$\mathrm{D}: \quad \Phi D(x,y,z) = \sin\omega x\sin\omega y\sin\omega z + \sin\omega x\cos\omega y\cos\omega z + \cos x\omega\sin\omega y\cos\omega z + \cos\omega x\cos\omega y\sin\omega z = c \tag{3}$$

where x, y, and z are spatial coordinates, $\omega = 2\pi/l$, and l is the length of the unit cell. By setting a 2π periodic domain, a unit cell with constant porosity is simply formed, and the domain is repeated along the three axes of the Cartesian coordinate system to form the entire structure. c is a constant. By changing c, the normal direction of the isosurface can be controlled, and the volume of the subdomain can be changed.

3 The impact of pore structure on the performance of TPMS

3.1 The influence of pore shape on the performance of TPMS bone scaffolds

3.1.1 The influence of pore shape on mechanical properties

In the domain of bone regeneration, the geometry and shape of the pore structure play a crucial role in determining the scaffold's mechanical properties [21]. By utilizing the periodic repetition of cubic translation cells, TPMS has successfully produced porous scaffolds with diverse pore geometric configurations [11]. Out of the various TPMS types, the Primitive(P), Gyroid(G), and (D) structures are the most common and thoroughly studied, as shown in Fig. 1A [22]. Each variant of TPMS exhibits unique morphological characteristics, with adjustable parameters to guarantee sufficient mechanical properties that can withstand physiological loads and provide necessary support to surrounding bone tissues [23]. A significant number of researchers focus on comparing the mechanical characteristics of these TPMS forms, which demonstrate remarkable mechanical traits regarding elastic modulus, yield strength, among others [24, 25]. This success is primarily linked to the geometric configuration of the TPMS, which enables precise modifications to the material's mechanical response by fine-tuning the pore shapes [26]. Kladovasilakis [27] successfully developed G, D, and P TPMS porous structures

A

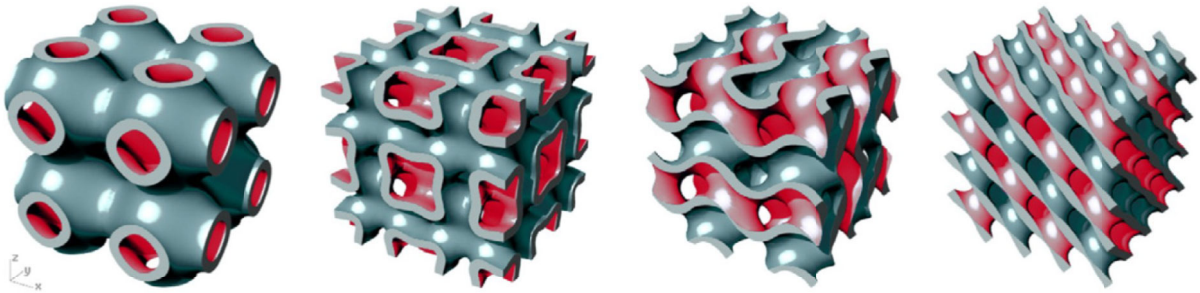

B

Type of Specimen	Effective Elastic Modulus Elat (MPa)	Compressive Yield Strength (Experimental) σ_{exp} (MPa)	Compressive Yield Strength (FEA) σ_{fea} (MPa)
Gyroid (ρ = 10%)	2708	27.33	27.11
Gyroid (ρ = 20%)	2804	39.82	39.89
Gyroid (ρ = 30%)	2928	55.76	53.55
Schwarz Diamond (ρ = 10%)	2624	24.17	25.83
Schwarz Diamond (ρ = 20%)	2685	42.52	39.32
Schwarz Diamond (ρ = 30%)	2896	56.67	51.71
Schwarz Primitive (ρ = 10%)	2250	15.44	17.61
Schwarz Primitive (ρ = 20%)	2334	25.15	33.63
Schwarz Primitive (ρ = 30%)	2713	41.11	47.50

C

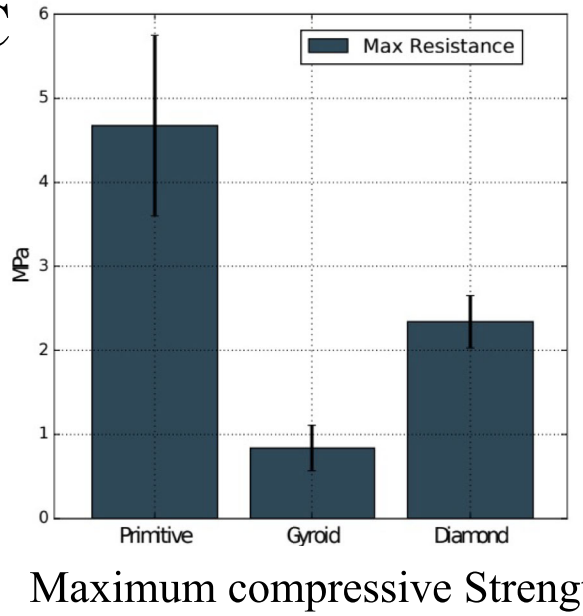

Table 2. TPMS's Young modulus.

TPMS	Porosity (%)	Young modulus (MPa)
Schwarz Primitive	$72.29441 \pm 1 \times 10^{-5}$	335.0
Gyroid	$81.73618 \pm 1 \times 10^{-5}$	51.7
Schwarz Diamond	$78.52382 \pm 1 \times 10^{-5}$	238.3

Fig. 1 **A** From left to right: P, I-WP, G, D. **B** Mechanical Properties of TPMS with Different Relative Densities. **C** Mechanical Properties of Different TPMS Structures

at varying relative densities of 10%, 20%, and 30% utilizing Fused Filament Fabrication (FFF) technology with Polylactic Acid (PLA). The results from compression tests indicated that, under equivalent relative density conditions, the D structure showcased the greatest mechanical strength, while the G structure followed closely, as depicted in Fig. 1B. Additionally, Restrepo [28] utilized 3D printing techniques to create ceramic models derived from TPMS. Their objective was to investigate the mechanical characteristics of G, P, and D structures across various TPMS

configurations to evaluate the feasibility of these models as scaffolds for bone tissue repair. As illustrated in Fig. 1C, the P design exhibited the most favorable mechanical traits regarding compressive strength and Young's modulus, aligning closely with the inherent properties of bone tissue. Through these studies, we have gained insights into the subtle differences in performance among different TPMS, which have sparked some discussion in the academic community. Although there is currently no consensus on which TPMS structure has superior performance, these studies undoubtedly provide valuable guidance for designing biomedical scaffolds that meet specific mechanical needs.

3.1.2 The influence of pore shape on biological performance

The shape of the pores significantly influences the permeability of bone scaffolds, and variations in permeability rates are associated with changes in pore morphology [27, 28]. In their study, Castro and colleagues [29] concentrated on assessing how the structural characteristics of three distinct TPMS bone scaffolds—designated as G, D, and P—affect their macroscopic permeability behavior. Utilizing Darcy's Law, the researchers computed the permeability of each scaffold via fluid dynamics testing. The results of the experiments, illustrated in Fig. 2A, align with theoretical predictions, indicating that decreased permeability rates occur at elevated flow rates. Specifically, the average difference in permeability between G70 (70% porosity of the G structure) and P70 (70% porosity of P structure) is 27%, while the difference between G70 and D70 (70% porosity of the D structure) is 49%. These findings reveal that the pore shape has a significant impact on the permeability rate, with the G structure showing a higher permeability rate and the D structure showing a lower permeability rate. The P structure exhibited the poorest permeability, which may imply its potential application value in promoting cell differentiation into osteoblasts. Therefore, bone scaffolds with G and D structures may become preferred candidate materials based on specific application requirements and the characteristics of the target bone tissue. The pore shape has a significant impact on the cell survival rate, migration rate, and bone regeneration efficiency of the TPMS structure of bone scaffolds [30, 31]. Liu and colleagues [32] manufactured size-gradient porous scaffolds with G and D structures using selective laser melting technology, demonstrating excellent in vitro biocompatibility. The experimental results, as shown in Fig. 2B, indicate that these scaffolds support the uniform adhesion and proliferation of osteoblasts, with the G structure scaffold showing better cell activity. The reason for this is that the G structure features a greater specific surface area, which facilitates easier cell penetration, enhances the smooth flow of the culture medium, and promotes better cell growth [33]. Such findings offer important implications for the development and production of orthopedic implants that possess enhanced bone integration and functional gradients. Montazerian and colleagues [34] manufactured three TPMS bone scaffold models of G, D, and P using the fused deposition printing technique. By encapsulating NIH-3T3 mouse fibroblast cells in the GelMA hydrogel of the scaffold and UV curing, the researchers found that the cell survival rate was above 90%, which was maintained for four days under culture conditions. These results demonstrate that the manufactured scaffolds are highly biocompatible in providing a suitable microenvironment for cells, making them strong candidate materials for tissue engineering applications. The configuration of pores additionally influences the scaffold's permeability and cellular biological activity, as the TPMS architecture enhances cell survival and proliferation owing to its greater specific surface area. These investigations offer crucial insights for refining the design of porous scaffolds, enhancing therapeutic outcomes, and satisfying physiological requirements.

3.2 The porosity affects the performance of the TPMS bone scaffold

3.2.1 The influence of porosity on mechanical properties

It is widely recognized that trabecular bone exhibits a porosity that varies between 50% and 90%, whereas cortical bone's porosity remains below 10% [34, 35]. Achieving a closer resemblance to natural bone structures necessitates careful control of porosity [36]. By modifying porosity levels, bone scaffolds can be designed to replicate either trabecular or cortical types, with variations possible depending on the specific anatomical region involved [37]. Additionally, matching the implant stiffness to that of the surrounding bone can mitigate complications associated with stress shielding [38, 39]. Consequently, porosity significantly influences the mechanical and biological characteristics of bone scaffolds [40]. In the context of porous architectures, a correlation known as the Gibson-Ashby relationship connects mechanical attributes to porosity levels [41]. A rise in porosity is associated with a decline in the internal solid structure, which ultimately results in diminished mechanical properties of TPMS bone scaffolds [42, 43]. Zhang [44] fabricated a G-structured TPMS bone scaffold using laser powder bed fusion (LPBF) with 316 L stainless steel powder. They assessed the compressive behavior of these scaffolds via Digital Image Correlation (DIC) and Finite Element Analysis (FEA) methods. The findings illustrated in Fig. 3A show that increasing TPMS

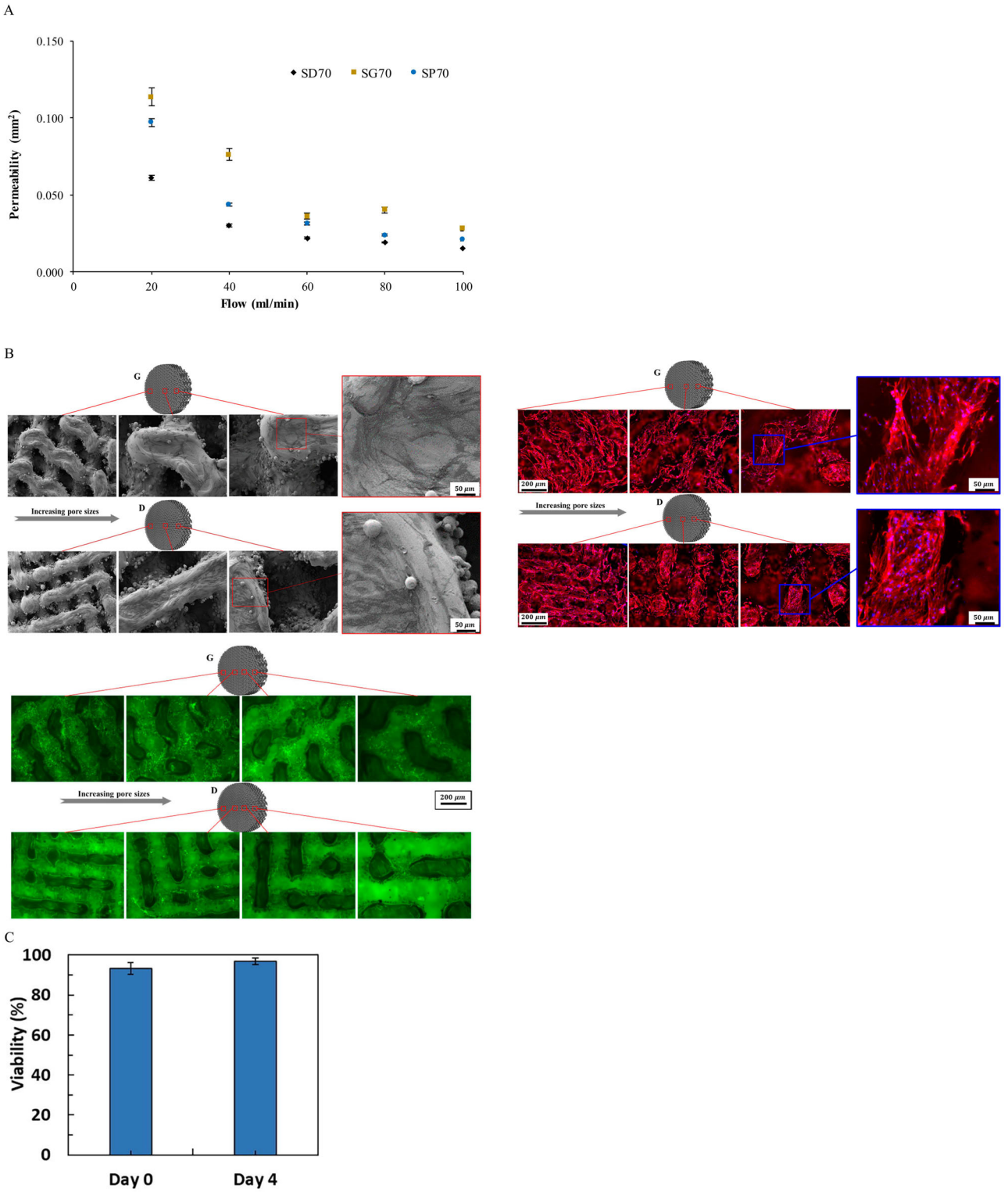

Fig. 2 **A** Investigate the relationship between the permeability rate and the flow velocity of the TPMS scaffold, while also considering the experimental standard deviation. **B** Three images depict the adhesion of osteoblasts on various scaffolds: SEM images reveal cell sizes from 0.6 to 2 millimeters, fluorescent images highlight cells with red actin filaments and blue cell nuclei, and images from FDA staining demonstrate cell viability. **C** The outcomes of cell viability assessments on day 0 and day 4

porosity leads to a gradual decline in both elastic modulus and compressive strength. Specifically, a 20% rise in porosity resulted in a 73% decrease in elastic modulus and an 85.8% reduction in compressive strength for the homogeneous TPMS. At elevated porosity levels, the Young's modulus of the TPMS bone scaffold approaches that of

A

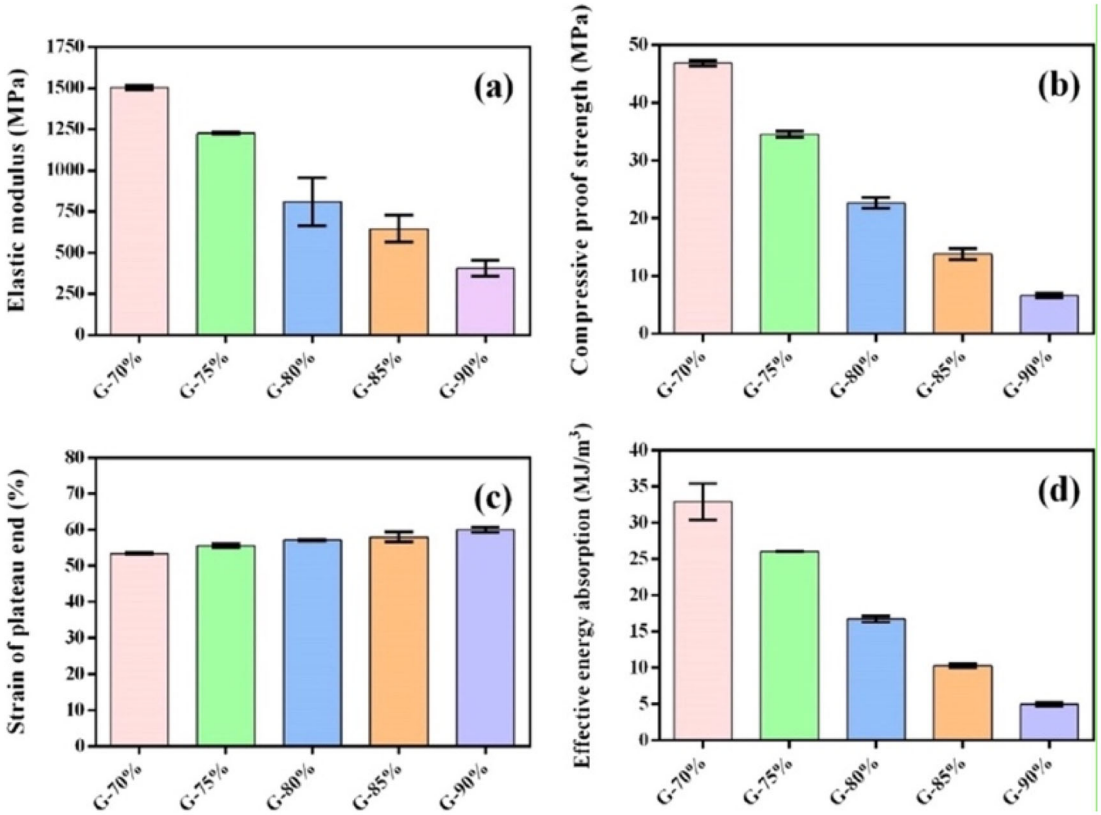

B

Lattice	Mechanical Properties	Porosity				
		40%	50%	60%	70%	80%
P	Effective Young's modulus (GPa)	21.66	16.02	11.24	7.26	4.21
	Compressive Yield stress (MPa)	237	185	139	97	56
G	Effective Young's modulus (GPa)	29.63	22.77	16.73	11.62	7.16
	Compressive Yield stress (MPa)	187	148	109	77	48

Fig. 3 **A** Properties related to the compression of homogeneous TPMS include: (a) elastic modulus, (b) proof strength under compression, (c) strain at the end of the plateau, and (d) the capacity for effective energy absorption. **B** The effective Young's modulus and the compressive strength were derived from the compression tests conducted on P and G lattice structures, which feature differing levels of porosity

trabecular bone. In a similar context, Verma [37] fabricated P and G bone scaffolds with porosities ranging from 40% to 80% using Ti6Al4V.The results of the numerical analysis illustrated in Fig. 3B highlight the effective Young's modulus and the compressive yield strength of P and G configurations throughout this porosity range. A higher porosity in the lattice structure leads to a decrease in Young's modulus along with a reduction in overall strength. Specifically, the effective modulus for the P configuration, observed at 80% porosity, is measured at 4.21 GPa, indicating approximately an 80% reduction when compared to the P configuration at 40% porosity. In the case of P

configurations with 80% porosity, the compressive yield strength is recorded at 56 MPa, which translates to around a 76% decline in comparison to the G configurations at 40% porosity. A similar trend is noted in the G configurations, where the effective Young's modulus falls from 29.63 GPa at 40% porosity to 7.16 GPa at 80% porosity, reflecting a reduction of about 75%. Additionally, the compressive yield strength shows a decrease of roughly 74% as porosity transitions from 40% to 80%. A study of the effective Young's modulus for both P and G configurations reveals a consistent decrease in the P structure. Conversely, the compressive yield strength of the G configuration tends to increase at all porosity levels, while the P configuration experiences a continuous decline. In summary, the mechanical characteristics of bone scaffolds are profoundly affected by porosity, which is vital for the progression of personalized medicine in the domain of bone tissue engineering. By carefully controlling porosity, it becomes feasible to effectively replicate the mechanical properties of different bone tissue types, thereby helping to mitigate issues such as stress shielding.

3.2.2 The influence of porosity on biological performance

Porosity significantly influences not only the mechanical characteristics of the scaffold but also the permeability of the TPMS scaffold, which varies at different rates with porosity, underlining its critical role. An elevated porosity level facilitates cell infiltration, vascular development, and effective nutrient diffusion [45]. Findings by Asbai-Ghoudan [46] indicate that at 90% porosity, the values for G and P structures are 4.3 and 6.2 times higher than those at 50% porosity, respectively, with the P structure generally exhibiting the highest permeability across most cases examined. However, in the 50% porosity model, G demonstrates the greatest permeability, as illustrated in Fig. 4A. Guerreiro [47] employed computational fluid dynamics (CFD) simulations to assess the permeability of three TPMS bone scaffolds, represented in Fig. 4B. The research revealed that increasing porosity from 50% to 60% results in approximately a 78% rise in the permeability of the P geometry, while a jump from 50% to 80% leads to around a 94% boost. For other models, the maximum increase was 72% (with comparable values for D and G), and P exhibited the most rapid enhancement in permeability among the three types. This variation may be attributed to pore distribution, wherein fluid flow behavior changes, alongside wall thickness, which can lead to alterations in flow channels and potential obstructions, culminating in greater pressure drops and reduced permeability in the structure. Currently, there is almost no research examining the permeability of TPMS porous structures that have porosity levels under 50%. Furthermore, the quantitative relationship between the structural parameters of TPMS and permeability has yet to be investigated [48]. Porous scaffolds facilitate efficient cell migration, attachment, proliferation, differentiation, and subsequent invasion, which contributes to vascularization. Additionally, they enhance the surface area that interacts with adjacent tissues [49]. Theoretically, increased porosity correlates with greater availability of space for cellular growth and movement; consequently, this enhances the potential for tissue repair, ultimately supporting new bone formation [50]. Extremely high or low porosity levels impede cell adhesion; excessive porosity diminishes the scaffold's surface area, which is not beneficial for cellular attachment, while insufficient porosity restricts the inward expansion of tissue cells [51]. Diez-Escudero [52] conducted a study on P, G, and D structures with porosities of 35%, 50%, and 65%, observing that all scaffolds exhibited low cell viability in the early stage due to inadequate seeding efficiency. Nonetheless, with the exception of the structure with 65% porosity, all geometric configurations permitted cell proliferation after 3 days of culture, achieving over 75% viability. Following a week, scaffolds exhibiting higher porosity demonstrated cell viability levels exceeding 100%. During the culture duration, cell proliferation rose in all scaffold structures, with the most notable improvement seen in the groups with 50% and 65% porosity, as shown in Fig. 4C. This highlights that the influence of pore size and distribution is more significant than that of interconnectivity. Although increased porosity may enhance cell migration and growth, it remains a challenge to preserve adequate mechanical strength. Thus, the choice of porosity influences bone regeneration outcomes indirectly due to its interplay with mechanical strength [53]. Therefore, it is essential to balance mechanical strength and porosity when designing bone scaffold engineering.

3.3 The influence of pore size on the performance of TPMS bone scaffolds

3.3.1 The influence of pore size on mechanical properties

The structure of human bones is characterized by a porous nature, which is marked by varying distributions and sizes of pores across different regions [54]. By employing a range of techniques to modify porosity, scaffolds can successfully replicate the pore size characteristics found in human skeletal frameworks [55]. An essential factor in the development of 3D-printed scaffolds for bone regeneration is the pore diameter [56]. The dimensions of the pores play a significant role in determining the compressive strength of these scaffolds [57]. Naghavi [58] performed experimental and numerical analyses to investigate the mechanical properties of scaffolds with G and D configurations, which exhibit varying pore sizes under compressive loads. The results, shown in Fig. 5A, indicate that a larger pore diameter leads to reductions in both the stiffness and yield strength of G and D scaffolds. For G scaffolds, the stiffness

A

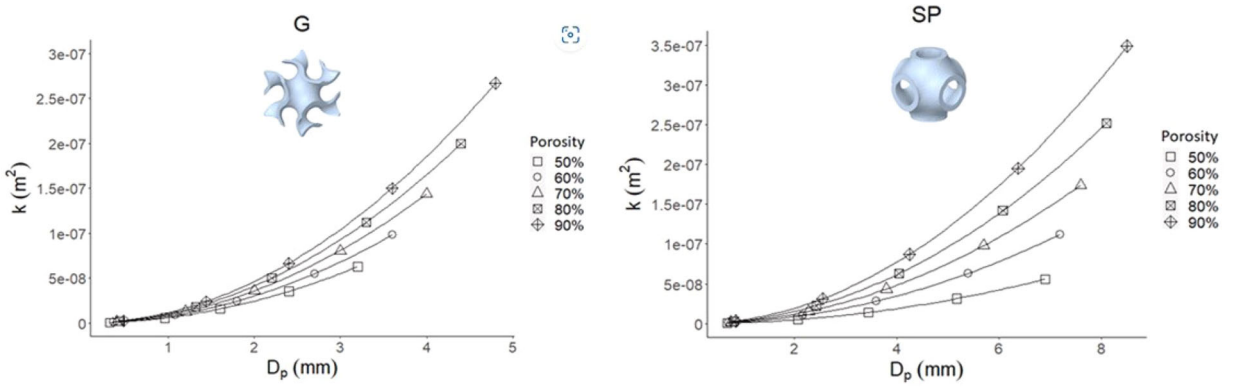

B

		Porosity							
		50%		60%		70%		80%	
	Method	HMG	CFD	HMG	CFD	HMG	CFD	HMG	CFD
Geometry	SD	3.51×10^{-3}	3.37×10^{-3}	5.79×10^{-3}	5.62×10^{-3}	8.96×10^{-3}	8.88×10^{-3}	1.27×10^{-2}	1.28×10^{-2}
	SG	5.86×10^{-3}	6.07×10^{-3}	9.75×10^{-3}	1.00×10^{-2}	1.46×10^{-2}	1.48×10^{-2}	2.11×10^{-2}	2.12×10^{-2}
	SP	1.19×10^{-3}	1.23×10^{-3}	5.35×10^{-3}	5.52×10^{-3}	1.20×10^{-2}	1.26×10^{-2}	2.08×10^{-2}	2.18×10^{-2}

C

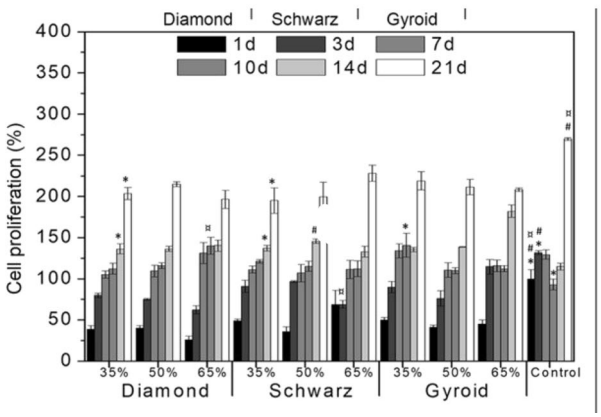

Fig. 4 **A** The correlation between porosity and permeability. **B** Permeability values (measured in mm^2) for various structures and their respective porosities, as determined through homogenisation (HMG) and computational fluid dynamics (CFD) analysis. SD represents D; SG indicates Gyroid; SP stands for P. **C** normalized with TCPS after 1 day of cell culture. Statistically significant differences among geometries at each time point with identical porosity ($p < 0.05$) are marked with * for 35%, # for 50%, and ¤ for 65%

and yield strength ranges, under designated pore diameter and porosity conditions, are between 4.40–9.54 GPa and 87–179 MPa, respectively; conversely, D scaffolds demonstrate ranges of 5.81–9.89 GPa and 106–170 MPa. It is worth mentioning that D scaffolds exhibit enhanced stiffness (~65% more) and strength (around 48% more) compared to G scaffolds under analogous porosity circumstances. Custom-designed scaffolds are intended to replicate the mechanical and physical characteristics of cortical bone, making them appropriate for use in orthopedic implants and bone replacement applications. A team led by Chen [59] presented a novel method that combines VAT photopolymerization with casting to create G structure bone scaffolds, with pore diameters of 650 µm, 800 µm, and 1040 µm, which are respectively abbreviated as G06, G08, and G10. Simulations suggested that the mechanical performance displayed by these porous scaffolds matched the experimental findings. Additionally, a thorough examination of the scaffolds' mechanical properties was conducted over a 90-day immersion duration to assess alterations related to degradation, offering a fresh perspective on evaluating the mechanical characteristics of porous scaffolds intended for bodily implantation, as shown in Fig. 5B. The variant with 650 µm pores demonstrated superior mechanical properties both prior to and following degradation in comparison to the scaffold with 1040 µm pores.

A

Test	Sample Name	Young's Modulus (GPa)			Yield Stress (MPa)		
		Experimental	Simulation	% Error	Experimental	Simulation	% Error
Compression	G600	8.46 ± 0.43	9.54	12%	181 ± 3	179	2%
	G800	6.81	6.96	2%	108	133	23%
	G1000	5.69	5.39	5%	94	105	12%
	D800	10.22 ± 0.31	10.78	5%	199 ± 3	183	8%
	D900	9.37	9.89	6%	159	170	7%
	D1100	7.59	8.06	6%	134	144	7%
	Cortical Bone	6–30	-	-	125–210	-	-

B

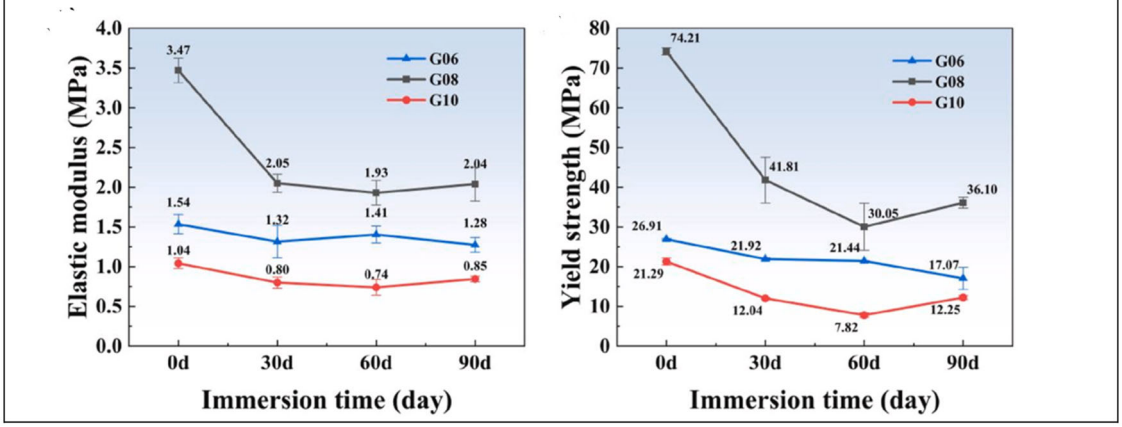

Fig. 5 **A** The mechanical properties of TPMS with different pore diameters under compression. **B** The change in the elastic modulus and yield strength of the bone scaffold with immersion time and degradation time

The scaffolds with 650 μm pores displayed remarkable biocompatibility and antimicrobial features, positioning them as excellent candidates for orthopedic applications. By meticulously managing the pore size, scaffolds exhibiting robust mechanical characteristics can be developed, which holds significant ramifications for bone regeneration and the enhancement of orthopedic implant technologies.

3.3.2 The influence of pore size on biological performance

The size of the pores is essential for influencing the permeability of bone scaffolds; variations in their diameter can impact permeability, with larger pore widths improving this property [60]. Research by Wang [61] employed computational fluid dynamics (CFD) to evaluate the permeability of P-structure bone scaffolds with pore diameters of 1100 μm, 900 μm, 700 μm, and 500 μm. The results indicated that larger pore sizes resulted in enhanced permeability, as demonstrated in Fig. 6A.This research suggests that the permeability of P-scaffolds is comparable to that of natural human bone $(0.5 < k(10^{-8}m^2) < 5)$, with the resulting flow characteristics potentially fostering tissue growth, thus presenting considerable opportunities for further research and application. Overall, pore size is essential in affecting cell migration, bone growth, and vascularization [62]. In one study by Ran [21], P-structure bone scaffolds with basic pore configurations (500, 700, and 900 μm) were engineered and fabricated through selective laser melting (SLM). Their research revealed that as pore diameter and porosity increased, the mechanical properties of the scaffolds weakened. While smaller pore diameters promote cell adhesion, larger diameters support cell proliferation; optimum bone tissue growth capability for the scaffold occurs at a pore diameter of 600 μm. With increasing pore size, the quantity of adhering cells rises correspondingly, and the abilities of cell proliferation and viability gradually improve, as depicted in Fig. 6B. This indicates that enhanced scaffold permeability facilitates cell infiltration, nutrient delivery, and waste elimination. Myakinin [63] developed bone scaffolds with P and D structures featuring pore diameters of 520 μm and 330 μm. As illustrated in Fig. 6C, their experimental findings indicated that the larger

pores of the 520 μm scaffold offered a greater number of attachment sites for cells compared to the 330 μm version. The diameter of pores within the porous structure is crucial for the inward growth of bone tissue [64]. At present, the ideal pore size in porous bone scaffolds remains a debated topic in the scientific community, larger pore sizes are not always advantageous, as excessively large pores might impair the interaction between cells and the scaffold material. In a related investigation, Guo [65] employed selective laser melting to fabricate Ti alloy scaffolds featuring a D structure, which were subsequently implanted in rabbits for in vivo experiments. Following a 12-week period, scaffolds characterized by a pore size of 500 μm demonstrated enhanced histological properties and increased collagen levels compared to their counterparts. Additionally, the fixation strength associated with the 500 μm pore scaffold was considerably higher than that of other implants. The influence of pore dimensions on the integration of soft tissue within these porous frameworks showed notable histological and biomechanical results, offering valuable insights for future research activities. Reduced pore sizes generally improve load-bearing capacity because they contribute to enhanced compressive strength; nonetheless, pore blockage can hinder the inward proliferation of bone tissue. Conversely, excessively large pores may limit the effective surface area, potentially affecting cell adhesion and consequently lowering the implant's load-bearing ability [55, 56]. Optimizing pore size or porosity could align more closely with the biomechanical characteristics of bone tissue, thereby improving the scaffold's biological efficacy [65]. The size of pores in the porous architecture significantly influences nutrient and blood flow, as well as cell adhesion, growth, interactions, and even the process of bone formation. Therefore, the appropriateness of the pore diameter serves as a crucial criterion for evaluating the porous structure [7]. Creating a pore diameter that balances both superior mechanical and biological properties is a challenging issue that remains to be completely addressed.

3.4 The influence of curvature on the performance of TPMS bone scaffolds

3.4.1 The influence of curvature on mechanical properties

TPMS denotes a surface that demonstrates periodic fluctuations across the X, Y, and Z axes within Euclidean space, exhibiting a zero average curvature and characteristics akin to the microstructure of trabecular bone [66]. Each version of this structure showcases a distinct periodic curvature distribution, which can be precisely modified to meet the specifications of particular target tissues [67, 68]. Yang [50] employed two methodologies, namely linear slip transformation (LST) and rotational slip transformation (RST), to effect morphological alterations in TPMS scaffolds, thus allowing for manipulation of their curvature distribution and Young's modulus. These strategies facilitate the creation of scaffolds with either symmetric or asymmetric curvature distributions, thereby expanding the spectrum of curvature within the lattice framework, which more accurately resembles the mechanical characteristics of trabecular bone. Modifying curvature significantly influences cell migration, as each TPMS setup offers a unique periodic surface curvature that can be tailored to the requirements of the target tissue [69]. Curvature serves as a critical element in assessing the degree of local surface deformation, and under consistent mechanical conditions, the micro-mechanical attributes of the structure are predominantly dictated by its surface curvature [70]. An in-depth examination of how curvature affects the stress conditions of structures is essential for comprehending the macroscopic mechanical properties of scaffolds. Yang [71] introduced a series of innovative G structure triply periodic minimal surface (TPMS) scaffolds that display a variety of average Gaussian curvatures, specifically $-2\,mm^{-2}$, $-4\,mm^{-2}$, and $-6\,mm^{-2}$, referred to as G2, G4, and G6, respectively. These structures were designed to achieve a porosity of 60%. In their research, a comparison was made between these novel scaffolds and traditional truss designs, both of which exhibited a porosity of 60%, but the latter were defined by a Gaussian curvature of 0, known as G0. As shown in Fig. 7A, their experimental results indicated that the TPMS bone scaffolds surpassed the G0 control regarding compressive strength. The measured compressive strengths were 61.93 ± 5.54 MPa for G2, 58.27 ± 4.05 MPa for G4, and 61.13 ± 4.45 MPa for G6, in contrast to the G0 control, which recorded a compressive strength of merely 37.67 ± 3.92 MPa. This significant difference in performance can be linked to the distinct design characteristics of the TPMS scaffolds, which effectively diminish stress concentration and improve load-bearing abilities during compression. Additionally, these TPMS scaffolds not only exhibit outstanding interconnectivity but also possess enhanced mechanical properties, positioning them as a promising choice for biomedical applications. In a noteworthy investigation, Li and colleagues [70] examined the mechanical properties of P-structure bone scaffolds, concentrating on the connection between local surface curvature and mechanical performance. The results are visually depicted in Fig. 7B, which shows the response of various local surfaces to applied loads. This figure indicates that when a uniform external force is applied to scaffolds with a curved surface positioned perpendicular to the load, a flatter surface results in greater local stress and deformation. Conversely, an increase in surface curvature generally leads to a decrease in local stress within the material. Additionally, the research suggests that when the surface supporting

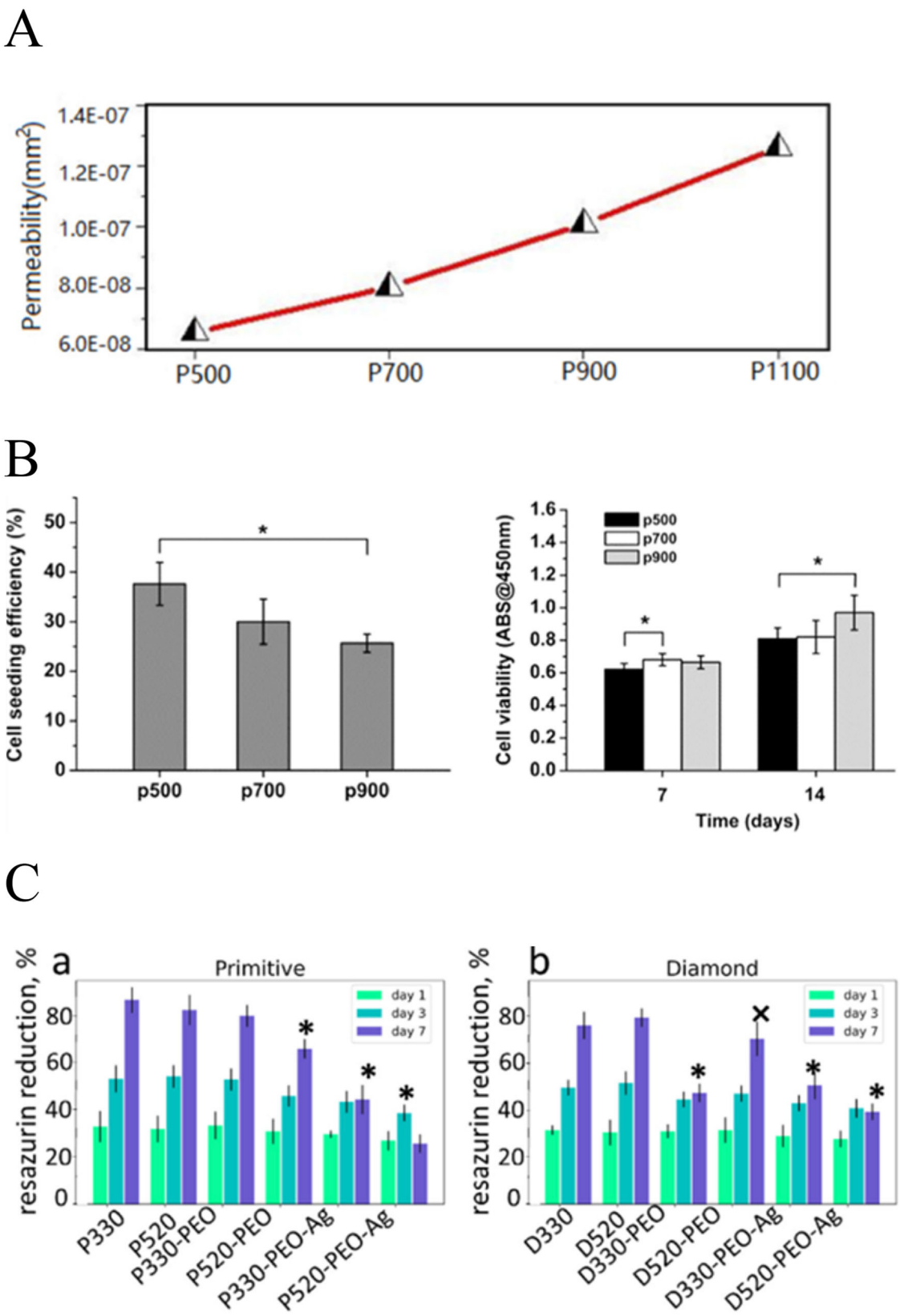

Fig. 6 **A** Permeability rates of different pore diameters. **B** Cell seeding efficiency and cell proliferation of bone scaffolds with different pore diameters. **C** Cell adhesion at different pore diameters over various days

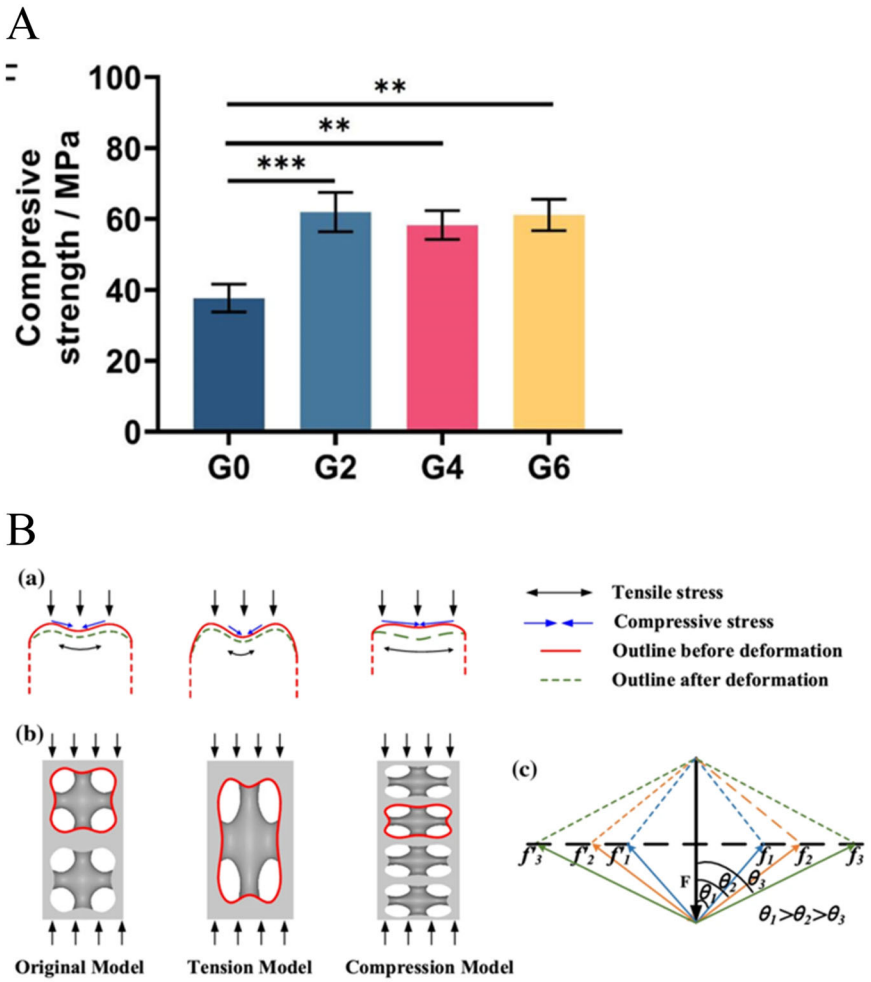

Fig. 7 **A** The compressive strength of TPMS scaffolds. **B** Connection between the curvature of the structure and its stress and deformation under loading: (a) the deformation and force state for various local surfaces; (b) curvature conditions of surfaces across different structures; (c) analysis of forces acting on surfaces with varying curvatures. Note: the length of the arrow indicates the intensity of the stress

the load is aligned parallel to the applied force, the flatter design demonstrates enhanced mechanical performance compared to its curved alternatives. These findings highlight the critical role of surface curvature in maximizing the mechanical behavior of bone scaffolds under different loading scenarios. Moreover, a curvature value approaching zero is linked to superior mechanical and fatigue resistance attributes. In summary, grasping how spatial angles and surface curvature influence the mechanical properties of scaffolds, along with developing models to predict these properties, will provide significant insights and further advancements in the design and evolution of bone scaffolds.

3.4.2 The influence of curvature on biological performance

Recent studies have increasingly focused on how curvature at the cellular level affects the behavior of cells and tissues [72]. This curvature significantly modifies the local biomechanical properties of structures, influencing cell proliferation, migration rates, and morphology on scaffold surfaces [70, 73]. Additionally, various cell types generally prefer localized concave surfaces over convex ones [74, 75]. The research conducted by Guo [76] focused on producing TPMS bone scaffolds featuring both P structure and G structure alongside Grid scaffolds. Their experimental results in cell culture showed that bone marrow stromal cells demonstrated improved adhesion, proliferation, and osteogenic differentiation when grown on the TPMS scaffolds. The configurations of the TPMS structures, whether concave or convex, are particularly effective in promoting tissue regeneration, as the cells are able to sense the curvature and differentiate within a specific range [77]. These results suggest that TPMS scaffolds possess considerable promise for use in bone repair applications. In a separate study, Yang [71] designed G TPMS scaffolds with average Gaussian curvatures of -2, -4, and $-6\,\mathrm{mm}^{-2}$ (designated as G2, G4, and G6), each having a porosity of 60%. These were evaluated against conventional truss scaffolds, which also exhibited 60% porosity but had a Gaussian curvature of 0, referred to as G0 for control comparison. Tests measuring cell viability on days 7, 14, and 28 revealed that the cell density (cells per surface area) on the curved surfaces G2, G4, and G6 was significantly higher than on the flat G0 surfaces, as demonstrated in Fig. 8A. The observed

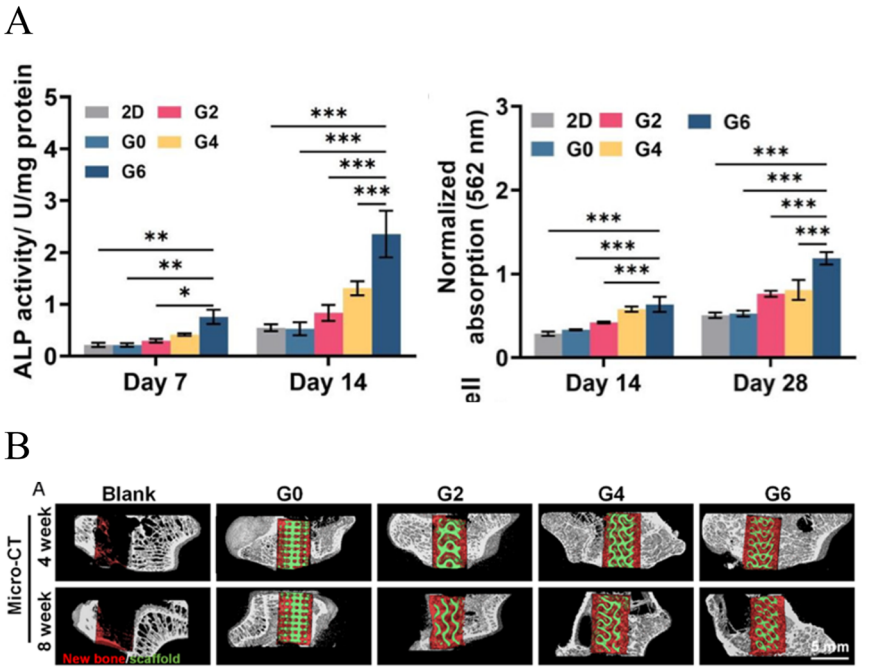

Fig. 8 **A** Quantification of hMSCs on day 7, day 14, and day 28. **B** 3D reconstructed images from micro-CT scans at 4 weeks and 8 weeks; red and green represent new bone tissue and the scaffold, respectively

enhancement may arise from the curved surfaces facilitating improved cell adhesion and retention rates, which indicates that TPMS scaffolds exhibit unique cytocompatibility [78]. The average curvature of these curved surfaces can affect the contractility of cells, thus influencing the growth behavior and morphology of bone-like tissue. Additionally, the role of curvature is vital in the regenerative mechanisms of bone tissue [50, 67]. Research has indicated that bone tissue tends to form preferentially on concave surfaces rather than on flat or convex surfaces. The study by Yang [71] explored the therapeutic benefits of using TPMS scaffolds for in vivo bone repair through a rabbit femoral defect model. They employed four scaffold variations, which included TPMS scaffolds exhibiting Gaussian curvatures of -2, -4, and $-6\,\mathrm{mm}^{-2}$, referred to as G2, G4, and G6, respectively, along with traditional truss scaffolds characterized by a Gaussian curvature of 0, serving as the control group (G0). Observations after 4 and 8 weeks of implantation revealed that new bone formation was considerably more pronounced in the TPMS scaffold groups than in the G0 control group. Furthermore, statistical evaluations demonstrated that the bone mineral density (BMD; 0.201 ± 0.021 g/cm³ and 0.365 ± 0.042 g/cm³) as well as the bone volume/total volume (BV/TV; 0.103 ± 0.017 and 0.174 ± 0.032) for the G6 group at both periods exceeded those of the other scaffolds, as depicted in Fig. 8B. An improvement in Gaussian curvature greatly enhanced the effectiveness of bone regeneration, leading to significant increases in BMD, BV/TV, and the development of new bone. This finding emphasizes the critical role that curvature plays in influencing bone regeneration. While the relationship between the mechanical properties of the TPMS structure and curvature remains somewhat ambiguous, research indicates that a lower curvature correlates with greater mechanical strength [70]. A TPMS surface exhibiting an average curvature of zero promotes better cell proliferation, effective nutrient transport, and efficient removal of metabolic waste [79]. Considering that the TPMS structure contains a periodically curved design, it is worthwhile to explore the latest generation of tissue engineering scaffolds developed from the TPMS, which highlights the significance of surface curvature in tissue engineering. By combining or interlocking surfaces with diverse distributions of surface curvature, these structures display a considerable degree of inherent complexity.

4 Effects of printing and materials on the performance of TPMS bone scaffolds

4.1 Effect of printing on the performance of TPMS bone scaffolds

TPMS structures cannot be accurately and efficiently prepared on a large scale by traditional manufacturing processes, while additive manufacturing (AM) is a technology that uses materials to stack layer by layer to produce solid components, and TPMS structures are manufactured. The commonly used methods for preparing TPMS structures are selective laser melting and selective laser sintering [21, 79]. During the additive manufacturing process, metal powders undergo a cycle of rapid heating and cooling, and the

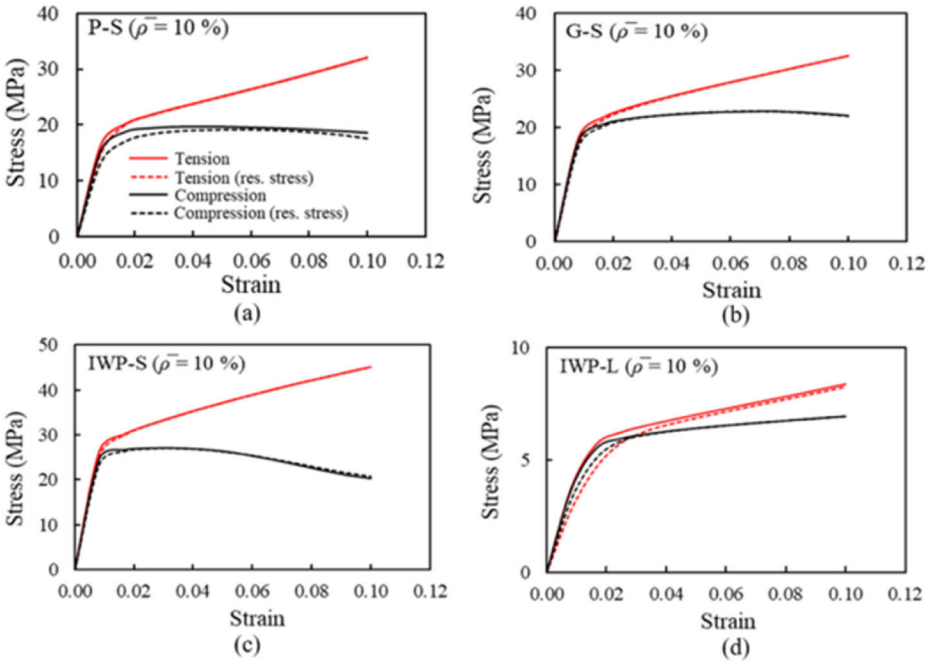

Fig. 9 Effect of residual stress on the tensile and compressive properties of TPMS structures. The stress–strain curve for tension/compression loading for $\rho = 10\%$ with and without residual stress: **a** P-S, **b** G-S, **c** IWP-S, and **d** IWP-L

uneven temperature field causes uneven plastic deformation. In the process of the temperature field returning to uniformity, due to the constraints of the surrounding materials, the material in the stress-existing area cannot expand and contract freely, which eventually leads to residual stress [80]. Based on the thermal-mechanical coupling finite element model, Ahmed [81] studied the residual stress generated during the SLM preparation of TPMS structures and its influence on the mechanical properties of TPMS structures. The simulation found that the TPMS structure will generate significant residual stress during the preparation process, and the residual stress has a great influence on the tensile and compression moduli of the structure (as shown in Fig. 9). Different topological structures of TPMS lead to different residual stress distributions, so its influence on the effective mechanical properties will vary depending on the topological structure. Mapari [82] studied the influence of residual stress on the compression properties of G-type and P-type TPMS structures. It was found that the simulation results considering residual stress are closer to the experimental data, which improves the simulation accuracy. The simulated stress-strain curve of the P-type structure is slightly higher than the experiment at 30% and 40% volume fractions, but slightly lower at 20%, which is related to the wall thickness error. The simulation results of the G-type structure are always lower than the experiment, which may be due to the increase in mass caused by manufacturing errors. Residual stress will reduce the elastic modulus and yield strength of the TPMS structure. The actual performance needs to consider factors such as residual stress and manufacturing errors. In the additive manufacturing process, the powder that is not completely melted forms a rough surface on the TPMS structure. The surface roughness has an important influence on the mechanical properties of the TPMS structure [83]. Yang [84] compared the stress-strain curves of the untreated and sandblasted skeleton G-type TPMS structure under quasi-static compression. The results show that after sandblasting, the elastic modulus, yield stress, and platform stress of the structure are increased by 5.9%, 9.3%, and 5.6% respectively compared with the TPMS structure with a rough surface. The above results show that the rough surface of the TPMS structure will reduce the compressive mechanical properties and fatigue fracture properties of the structure. In summary, additive manufacturing technology makes it possible to manufacture complex TPMS structures, but the residual stress and surface roughness generated during the manufacturing process have a significant effect on the mechanical properties of the structure. Therefore, these factors need to be considered when designing and manufacturing TPMS structures to optimize their performance.

4.2 Effect of materials on the performance of TPMS bone scaffolds

The inherent properties of materials can significantly affect cell diffusion behavior, thereby regulating the volume and spatial distribution of regenerated bone tissue [85]. Shen [86] fabricated a series of Mg-doped wollastonite TPMS bone scaffolds. The TPMS-based scaffolds were fabricated and tested in vitro for morphology, mechanical properties, and biocompatibility, and finally implanted in vivo. The

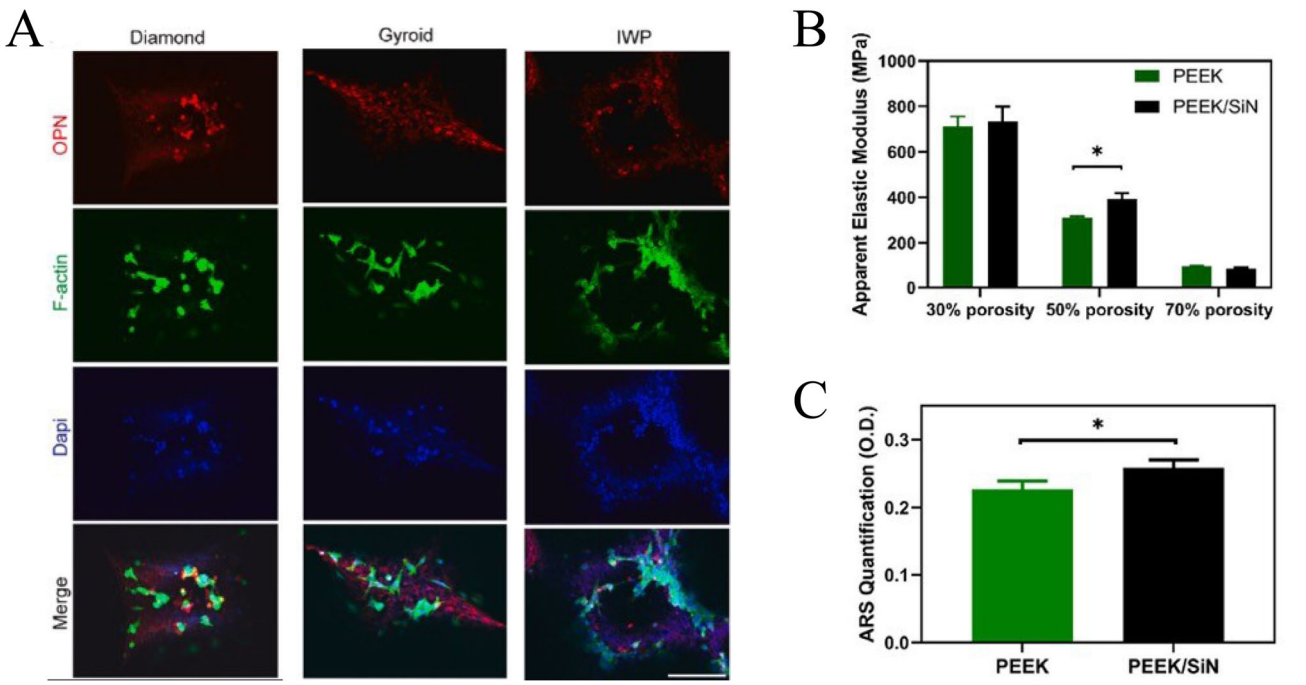

Fig. 10 **A** Immunofluorescence staining of OPN in BMSCs seeded on different scaffolds after 7 days of incubation. **B** Apparent elastic modulus of PEEK and PEEK/SiN scaffolds with different porosities under vertical compression. **C** Quantitative analysis of mineralization by Alizarin Red S (ARS) staining after 10 days

results showed that compared with the I-WP bone scaffold, the initial compressive strength of Diamond and Gyroid increased by 3–4 times, and the magnesium ion release rate increased by 20–40%. As shown in Fig. 10A, the use of bioceramics increased the expression of osteoblasts, especially for Diamond and Gyroid. The design method in the study provides an important perspective for optimizing the pore structure design of bioceramic scaffolds to accelerate osteogenesis and promote the clinical transformation of bioceramic scaffolds in bone repair. However, the biggest disadvantage of this material is that it is too brittle, and the structural properties of TPMS can partially alleviate their brittleness. Baumer [14] used a low-cost technology that combined robotic casting with layered photopolymerization to successfully print hydroxyapatite TPMS scaffolds. The porosity was 74.05%, which is within the optimal range for bone tissue creation. This TPMS scaffold provides structural quality to compensate for material defects and alleviate the brittleness of hydroxyapatite. Du [87] fabricated PEEK and PEEK/SiN bone scaffolds with tri-periodic minimum surface (TPMS) structures by 3D printing technology and analyzed and compared their properties by performing mechanical tests and biological experiments on these scaffolds. As shown in Fig. 10B, C, the PEEK/SiN bone scaffold outperformed the PEEK bone scaffold in terms of mechanical properties, and the PEEK/SiN scaffold showed significantly higher calcium deposition, indicating a higher degree of mineralization. This result suggests that the incorporation of silicon nitride into the PEEK scaffold can stimulate the differentiation of osteoblasts. Based on these findings, it can be inferred that the PEEK/SiN TPMS scaffold has great application potential in the field of bone tissue engineering. In summary, these studies show that by optimizing material selection, the performance of bone scaffolds can be significantly improved, the rate of osteogenesis can be accelerated, and its clinical application in bone repair can be promoted.

5 Conclusion

Owing to the remarkable effectiveness of TPMS bone scaffolds, they are increasingly recognized as a significant approach in bone tissue engineering aimed at treating femoral head necrosis. In the past few years, TPMS bone scaffolds' performance has garnered considerable attention in research. The objective of the design is to create TPMS models that mimic the structural features of natural bone, thereby providing distinct mechanical and biological properties suitable for diverse application scenarios. The efficacy of TPMS bone scaffolds is primarily demonstrated through their mechanical and biological attributes. By manipulating the implicit function and its parameters, performance adjustments can be made, with factors such as pore shape, porosity, pore size, and curvature playing crucial roles in the scaffolds' overall performance. To better suit the

implantation site, modifying these parameters can significantly diminish the scaffolding structure's mechanical properties, including compressive stress, yield stress, and elastic modulus, all of which are influenced by the pore architecture, thus helping to mitigate or even eliminate stress shielding. The scaffold's permeability and pore interconnectivity can be modified to enhance nutrient transport and facilitate metabolic waste removal, thereby improving biological performance and promoting cell adhesion, proliferation, and growth. Additionally, it aids in guiding bone ingrowth, leading to superior osseointegration outcomes, which are crucial for effective early bone regeneration and long-term structural integrity. It is evident that the pore structure design of the scaffold primarily influences bone tissue repair. Despite the increasing depth of current research on TPMS bone scaffolds, detailed correlations between their pore configurations and mechanical properties remain insufficient. The inherent complexity of natural bone geometry and the variability in its characteristics present challenges in locally controlling internal pore attributes to fit the needs of specific repair sites. While numerous investigations have assessed how pore structure parameters affect porous scaffolds, achieving precise adjustments to meet specific demands remains challenging, and no universal standards have been established for the fabrication of biomimetic porous scaffolds intended for clinical use. By optimizing material selection and combining additive manufacturing technology, and fully considering defects introduced during the manufacturing process, the performance of bone scaffolds can be significantly improved, bone tissue regeneration can be accelerated, and its application in clinical bone repair can be promoted. Consequently, optimizing the performance of TPMS bone scaffolds is a pressing issue in contemporary research. Comprehensive and in-depth studies are essential to develop a more scientific and effective selection criterion for TPMS scaffolds, which would provide dependable support and guidance for their use in orthopedic clinical settings.

Author contributions Yadi Sun: Conceptualization, investigation, Writing–original draft, Reviewing and Editing.Yan Wang and Benchao Dong: Data curation, Investigation, Project administration, Reviewing and Editing.Peichuan Yang: Reviewing and Editing.Chunhui Ji and Yiyang Li: Data curation, Investigation, Reviewing and Editing.Jianxiong Ma and Xinlong Ma: Conceptualization, Funding acquisition, Project administration, and Reviewing.

Funding This work was supported by grants from the National Key Research and Development Program (No. 2022YFC3601900), the Key Project of Natural Science Foundation of Tianjin (No. 22JCZDJC00340), the Tianjin Health and Health Technology Project (No. TJWJ2022QN053), the National Natural Science Foundation of China (No. 32271432), and the National Natural Science Foundation of China (No. 82405109).

Compliance with ethical standards

Conflict of interest The authors declare no competing interests.

Publisher's note Springer Nature remains neutral with regard to jurisdictional claims in published maps and institutional affiliations.

References

1. Ma Z, Yang Q, Liu X, Li Z. Application of allograft and absorbable screws in the reconstruction of a massive bone defect following resection of giant osteochondroma: a retrospective study. Front Surg. 2022;9:938750.
2. Feltri P, Solaro L, Errani C, Schiavon G, Candrian C, Filardo G. Vascularized fibular grafts for the treatment of long bone defects: pros and cons. A systematic review and meta-analysis. Arch Orthop Trauma Surg. 2023;143:29–48.
3. Alonzo M, Alvarez Primo F, Anil Kumar S, Mudloff JA, Dominguez E, Fregoso G, et al. Bone tissue engineering techniques, advances, and scaffolds for treatment of bone defects. Curr Opin Biomed Eng. 2021;17:100248.
4. Wang H, Yu H, Huang T, Wang B, Xiang L. Hippo-YAP/TAZ signaling in osteogenesis and macrophage polarization: therapeutic implications in bone defect repair. Genes Dis. 2023;10:2528–39.
5. Gens L, Marchionatti E, Steiner A, Stoddart MJ, Thompson K, Mys K, et al. Surgical technique and comparison of autologous cancellous bone grafts from various donor sites in rats. J Orthop Res Off Publ Orthop Res Soc. 2023;41:834–44.
6. Feng B, Zhang M, Qin C, Zhai D, Wang Y, Zhou Y, et al. 3D printing of conch-like scaffolds for guiding cell migration and directional bone growth. Bioact Mater. 2023;22:127–40.
7. Zhao L, Pei X, Jiang L, Hu C, Sun J, Xing F, et al. Bionic design and 3D printing of porous titanium alloy scaffolds for bone tissue repair. Compos Part B Eng. 2019;162:154–61.
8. Wu J, Zhang Y, Lyu Y, Cheng L. On the various numerical techniques for the optimization of bone scaffold. Materials. 2023;16:974.
9. Zhang J, Shen Y, Sun Y, Yang J, Gong Y, Wang K, et al. Design and mechanical testing of porous lattice structure with independent adjustment of pore size and porosity for bone implant. J Mater Res Technol. 2022;18:3240–55.

10. Sun J, Zhang Y, Wang Y. Application of minimal curved surface in the design and preparation of bone scaffold. In: 2021 International Conference on Machine Learning and Intelligent Systems Engineering (MLISE) (p. 521–5). IEEE; 2021.
11. Maevskaia E, Guerrero J, Ghayor IWFE. Triply periodic minimal surface-based scaffolds for bone tissue engineering: a mechanical, in vitro and in vivo study. Tissue Eng, Part A. 2023;29:507–17.
12. Bobbert FSL, Lietaert K, Eftekhari AA, Pouran B, Ahmadi SM, Weinans H, et al. Additively manufactured metallic porous biomaterials based on minimal surfaces: a unique combination of topological, mechanical, and mass transport properties. Acta Biomater. 2017;53:572–84.
13. Jia H, Lei H, Wang P, Meng J, Li C, Zhou H, et al. An experimental and numerical investigation of compressive response of designed Schwarz Primitive triply periodic minimal surface with non-uniform shell thickness. Extrem Mech Lett. 2020;37:100671.
14. Baumer V, Gunn E, Riegle V, Bailey C, Shonkwiler C, Prawel D. Robocasting of ceramic Fischer–Koch S Scaffolds for bone tissue engineering. J Funct Biomater. 2023;14:251.
15. Li J, Xu Z, Wang Q, Hu G, Wang Y. Coupling control of pore size and spatial distribution in bone scaffolds based on a random strategy for additive manufacturing. Rapid Prototyp J. 2019;25:1030–44.
16. Feng J, Fu J, Shang C, Lin Z, Niu X, Li B. Efficient generation strategy for hierarchical porous scaffolds with freeform external geometries. Addit Manuf. 2020;31:100943.
17. Wang G, Shen L, Zhao J, Liang H, Xie D, Tian Z, et al. Design and compressive behavior of controllable irregular porous scaffolds: based on Voronoi-tessellation and for additive manufacturing. ACS Biomater Sci Eng. 2018;4:719–27.
18. Gupta A, Babu S. "Triply periodic minimal surfaces: an overview of their features, failure mechanisms, and applications." J Mines Metals Fuels. 2022:211–21.
19. Do Carmo, MP. Differential geometry of curves and surfaces: revised and updated second edition. Courier Dover Publications; 2016.
20. Xi H, Zhou Z, Zhang H, Huang S, Xiao H. Multi-morphology TPMS structures with multi-stage yield stress platform and multi-level energy absorption: design, manufacturing, and mechanical properties. Eng Struct. 2023;294:116733.
21. Ran Q, Yang W, Hu Y, Shen X, Yu Y, Xiang Y, et al. Osteogenesis of 3D printed porous Ti6Al4V implants with different pore sizes. J Mech Behav Biomed Mater. 2018;84:1–11.
22. Li Y, Li J, Jiang S, Zhong C, Zhao C, Jiao Y, et al. The design of strut/TPMS-based pore geometries in bioceramic scaffolds guiding osteogenesis and angiogenesis in bone regeneration. Mater Today Bio. 2023;20:100667.
23. Han L, Che S. An overview of materials with triply periodic minimal surfaces and related geometry: from biological structures to self-assembled systems. Adv Mater. 2018;30:1705708.
24. Maconachie T, Leary M, Lozanovski B, Zhang X, Qian M, Faruque O, et al. SLM lattice structures: Properties, performance, applications and challenges. Mater Des. 2019;183:108137.
25. Mustafa NS, Akhmal NH, Izman S, Ab Talib MH, Shaiful AIM, Omar MNB, et al. Application of computational method in designing a unit cell of bone tissue engineering scaffold: a review. Polymers. 2021;13:1584.
26. Zhao M, Liu F, Fu G, Zhang DZ, Zhang T, Zhou H. Improved mechanical properties and energy absorption of BCC lattice structures with triply periodic minimal surfaces fabricated by SLM. Materials. 2018;11:2411.
27. Kladovasilakis N, Tsongas K, Tzetzis D. Mechanical and FEA-assisted characterization of fused filament fabricated triply periodic minimal surface structures. J Compos Sci. 2021;5:58.
28. Restrepo S, Ocampo S, Ramírez JA, Paucar C, García C. Mechanical properties of ceramic structures based on Triply Periodic Minimal Surface (TPMS) processed by 3D printing. J Phys Conf Ser. 2017;935:012036.
29. Santos J, Pires T, Gouveia BP, Castro APG, Fernandes PR. On the permeability of TPMS scaffolds. J Mech Behav Biomed Mater. 2020;110:103932.
30. Castro APG, Pires T, Santos JE, Gouveia BP, Fernandes PR. Permeability versus design in TPMS scaffolds. Materials. 2019;12:1313.
31. Kim J-W, Yang B-E, Hong S-J, Choi H-G, Byeon S-J, Lim H-K, et al. Bone regeneration capability of 3D printed ceramic scaffolds. Int J Mol Sci. 2020;21:4837.
32. Flores-Jiménez MS, Garcia-Gonzalez A, Fuentes-Aguilar RQ. Review on porous scaffolds generation process: a tissue engineering approach. ACS Appl Bio Mater. 2023;6:1–23.
33. Liu F, Ran Q, Zhao M, Zhang T, Zhang DZ, Su Z. Additively manufactured continuous cell-size gradient porous scaffolds: pore characteristics, mechanical properties and biological responses in vitro. Materials. 2020;13:2589.
34. Montazerian H, Mohamed MGA, Montazeri MM, Kheiri S, Milani AS, Kim K, et al. Permeability and mechanical properties of gradient porous PDMS scaffolds fabricated by 3D-printed sacrificial templates designed with minimal surfaces. Acta Biomater. 2019;96:149–60.
35. Cai Z, Liu Z, Hu X, Kuang H, Zhai J. The effect of porosity on the mechanical properties of 3D-printed triply periodic minimal surface (TPMS) bioscaffold. Bio-Des Manuf. 2019;2:242–55.
36. Fantini M, Curto M, De Crescenzio F. TPMS for interactive modelling of trabecular scaffolds for bone tissue engineering: 8th International Joint Conference on Mechanics, Design Engineering and Advanced Manufacturing. Eynard B, Nigrelli V, Oliveri SM, Peris-Fajarnes G, Rizzuti S, editors. Advances on Mechanics, Design Engineering and Manufacturing. 2017;425–35.
37. Verma R, Kumar J, Singh NK, Rai SK, Saxena KK, Xu J. Design and analysis of biomedical scaffolds using TPMS-based porous structures inspired from additive manufacturing. Coatings. 2022;12:839.
38. Gunther F, Wagner M, Pilz S, Gebert A, Zimmermann M. Design procedure for triply periodic minimal surface based biomimetic scaffolds. J Mech Behav Biomed Mater. 2022;126:104871.
39. Yang L, Mertens R, Ferrucci M, Yan C, Shi Y, Yang S. Continuous graded Gyroid cellular structures fabricated by selective laser melting: design, manufacturing and mechanical properties. Mater Des. 2019;162:394–404.
40. Yuan L, Ding S, Wen C. Additive manufacturing technology for porous metal implant applications and triple minimal surface structures: a review. Bioact Mater. 2019;4:56–70.
41. Montazerian H, Davoodi E, Asadi-Eydivand M, Kadkhodapour J, Solati-Hashjin M. Porous scaffold internal architecture design based on minimal surfaces: a compromise between permeability and elastic properties. Mater Des. 2017;126:98–114.
42. Uhlířová T, Pabst W. Conductivity and Young's modulus of porous metamaterials based on Gibson-Ashby cells. Scr Mater. 2019;159:1–4.
43. Kumar J, Verma R, Singh NK, Singh NK, Nirala NS, Rai SK. Mechanical property analysis of triply periodic minimal surface inspired porous scaffold for bone applications: a compromise between desired mechanical strength and additive manufacturability. J Mater Eng Perform. 2023;32:3335–47.
44. Zhang M, Li J, Liao X, Xu M, Shi W. Influence of cycle number on the compression behavior of nonlinear periodically gradient porous structures produced by laser powder bed fusion. Mater Des. 2022;223:111257.
45. Roseti L, Parisi V, Petretta M, Cavallo C, Desando G, Bartolotti I, et al. Scaffolds for bone tissue engineering: state of the art and new perspectives. Mater Sci Eng C. 2017;78:1246–62.

46. Asbai-Ghoudan R, Ruiz de Galarreta S, Rodriguez-Florez N. Analytical model for the prediction of permeability of triply periodic minimal surfaces. J Mech Behav Biomed Mater. 2021;124:104804.
47. Guerreiro R, Pires T, Guedes JM, Fernandes PR, Castro APG. On the tortuosity of TPMS scaffolds for tissue engineering. Symmetry-Basel. 2020;12:596.
48. Zeng C, Wang W. Modeling method for variable and isotropic permeability design of porous material based on TPMS lattices. Tribol Int. 2022;176:107913.
49. Liu S, Qin S, He M, Zhou D, Qin Q, Wang H. Current applications of poly(lactic acid) composites in tissue engineering and drug delivery. Compos Part B Eng. 2020;199:108238.
50. Yang N, Wei H, Mao Z. Tuning surface curvatures and Young's moduli of TPMS-based lattices independent of volume fraction. Mater Des. 2022;216:110542.
51. Wang Z, Yao R, Wang D, Wang H, Liang C. Structure design and biological evaluation of the mechanical-adaptive titanium-based porous implants. Mater Technol. 2021;36:851–6.
52. Diez-Escudero A, Harlin H, Isaksson P, Persson C. Porous polylactic acid scaffolds for bone regeneration: a study of additively manufactured triply periodic minimal surfaces and their osteogenic potential. J Tissue Eng. 2020;11:2041731420956541.
53. Dong Z, Zhao X. Application of TPMS structure in bone regeneration. Eng Regen. 2021;2:154–62.
54. Onal E, Frith JE, Jurg M, Wu X, Molotnikov A. Mechanical properties and in vitro behavior of additively manufactured and functionally graded Ti6Al4V porous scaffolds. Metals. 2018;8:200.
55. Lv Y, Liu G, Wang B, Tang Y, Lin Z, Liu J, et al. Pore strategy design of a novel NiTi-Nb biomedical porous scaffold based on a triply periodic minimal surface. Front Bioeng Biotechnol. 2022;10:910475.
56. Zhang L, Yang G, Johnson BN, Jia X. Three-dimensional (3D) printed scaffold and material selection for bone repair. Acta Biomater. 2019;84:16–33.
57. Zhang Q, Ma L, Ji X, He Y, Cui Y, Liu X, et al. High-strength hydroxyapatite scaffolds with minimal surface macrostructures for load-bearing bone regeneration. Adv Funct Mater. 2022;32:2204182.
58. Naghavi SA, Tamaddon M, Marghoub A, Wang K, Babamiri BB, Hazeli K, et al. Mechanical characterisation and numerical modelling of TPMS-based gyroid and Ti6Al4V scaffolds for bone implants: an integrated approach for translational consideration. Bioengineering. 2022;9:504.
59. Chen B, Sun X, Liu D, Tian H, Gao J. A novel method combining VAT photopolymerization and casting for the fabrication of biodegradable zn-1Mg scaffolds with triply periodic minimal surface. J Mech Behav Biomed Mater. 2023;141:105763.
60. Ali D, Ozalp M, Blanquer SBG, Onel S. Permeability and fluid flow-induced wall shear stress in bone scaffolds with TPMS and lattice architectures: a CFD analysis. Eur J Mech B Fluids. 2020;79:376–85.
61. Wang S, Shi Z, Liu L, Zhou X, Zhu L, Hao Y. The design of Ti6Al4V primitive surface structure with symmetrical gradient of pore size in biomimetic bone scaffold. Mater Design. 2020;193:108830.
62. Hsieh M-T, Begley MR, Valdevit L. Architected implant designs for long bones: advantages of minimal surface-based topologies. Mater Des. 2021;207:109838.
63. Myakinin A, Turlybekuly A, Pogrebnjak A, Mirek A, Bechelany M, Liubchak I, et al. In vitro evaluation of electrochemically bioactivated Ti6Al4V 3D porous scaffolds. Mater Sci Eng C-Mater Biol Appl. 2021;121:111870.
64. Li L, Wang P, Liang H, Jin J, Zhang Y, Shi J, et al. Design of a haversian system-like gradient porous scaffold based on triply periodic minimal surfaces for promoting bone regeneration. J Adv Res. 2023;S2090-1232(23)00004–8.
65. Guo Y, Liu F, Bian X, Lu K, Huang P, Ye X, et al. Effect of pore size of porous-structured titanium implants on tendon ingrowth. Appl Bionics Biomech. 2022;2022:2801229.
66. Ouyang P, Dong H, He X, Cai X, Wang Y, Li J, et al. Hydromechanical mechanism behind the effect of pore size of porous titanium scaffolds on osteoblast response and bone ingrowth. Mater Des. 2019;183:108151.
67. Blanquer SBG, Werner M, Hannula M, Sharifi S, Lajoinie GPR, Eglin D, et al. Surface curvature in triply-periodic minimal surface architectures as a distinct design parameter in preparing advanced tissue engineering scaffolds. Biofabrication. 2017;9:025001.
68. Kelly CN, Lin AS, Leguineche KE, Shekhar S, Walsh WR, Guldberg RE, et al. Functional repair of critically sized femoral defects treated with bioinspired titanium gyroid-sheet scaffolds. J Mech Behav Biomed Mater. 2021;116:104380.
69. Li Z, Chen Z, Chen X, Zhao R. Effect of surface curvature on the mechanical and mass-transport properties of additively manufactured tissue scaffolds with minimal surfaces. Acs Biomater Sci Eng. 2022;8:1623–43.
70. Li Z, Chen Z, Chen X, Zhao R. Mechanical properties of triply periodic minimal surface (TPMS) scaffolds: Considering the influence of spatial angle and surface curvature. Biomech Modeling Mechanobiol. 2022;22:541–60.
71. Yang Y, Xu T, Bei H-P, Zhang L, Tang C-Y, Zhang M, et al. Gaussian curvature–driven direction of cell fate toward osteogenesis with triply periodic minimal surface scaffolds. Proc Natl Acad Sci USA. 2022;119:e2206684119.
72. Callens SJP, Fan D, van Hengel IAJ, Minneboo M, Díaz-Payno PJ, Stevens MM, et al. Emergent collective organization of bone cells in complex curvature fields. Nat Commun. 2023;14:855.
73. Callens SJP, Uyttendaele RJC, Fratila-Apachitei LE, Zadpoor AA. Substrate curvature as a cue to guide spatiotemporal cell and tissue organization. Biomaterials. 2020;232:119739.
74. Bade ND, Xu T, Kamien RD, Assoian RK, Stebe KJ. Gaussian curvature directs stress fiber orientation and cell migration. Biophys J. 2018;114:1467–76.
75. Pieuchot L, Marteau J, Guignandon A, Dos Santos T, Brigaud I, Chauvy P-F, et al. Curvotaxis directs cell migration through cell-scale curvature landscapes. Nat Commun. 2018;9:1–13.
76. Guo W, Yang Y, Liu C, Bu W, Guo F, Li J, et al. 3D printed TPMS structural PLA/GO scaffold: process parameter optimization, porous structure, mechanical and biological properties. J Mech Behav Biomed Mater. 2023;142:105848.
77. Zhang J, Chen X, Sun Y, Yang J, Chen R, Xiong Y, et al. Design of a biomimetic graded TPMS scaffold with quantitatively adjustable pore size. Mater Des. 2022;218:110665.
78. Ali D. Effect of scaffold architecture on cell seeding efficiency: a discrete phase model CFD analysis. Comput Biol Med. 2019;109:62–9.
79. Ma S, Tang Q, Han X, Feng Q, Song J, Setchi R, et al. Manufacturability, mechanical properties, mass-transport properties and biocompatibility of triply periodic minimal surface (TPMS) porous scaffolds fabricated by selective laser melting. Mater Des. 2020;195:109034.
80. Wu J, Wang L, An X. Numerical analysis of residual stress evolution of AlSi10Mg manufactured by selective laser melting. Optik. 2017;137:65–78.
81. Ahmed N, Barsoum I, Abu ARK. Numerical investigation on the effect of residual stresses on the effective mechanical properties of 3D-printed TPMS lattices. Metals. 2022;12:1344.
82. Mapari HS, Kruse H, Escobar de Obaldia E; Matei A, Schleifenbaum JH. Effect of residual stresses on the mechanical properties of additive manufactured TPMS lattice structures made of

stainless steel. Aachen: Universitätsbibliothek der RWTH Aachen. 2023:2–13.
83. Günther F, Hirsch F, Pilz S, Wagner M, Gebert A, Kästner M, et al. Structure-property relationships of imperfect additively manufactured lattices based on triply periodic minimal surfaces. Mater Des. 2022;222:111036.
84. Yang L, Yan C, Cao W, Liu Z, Song B, Wen S, et al. Compression–compression fatigue behaviour of gyroid-type triply periodic minimal surface porous structures fabricated by selective laser melting. Acta Mater. 2019;181:49–66.
85. Asbai-Ghoudan R, Nasello G, Pérez MÁ, Verbruggen SW, Ruiz de Galarreta S, Rodriguez-Florez N. In silico assessment of the bone regeneration potential of complex porous scaffolds. Comput Biol Med. 2023;165:107381.
86. Shen M, Li Y, Lu F, Gou Y, Zhong C, He S, et al. Bioceramic scaffolds with triply periodic minimal surface architectures guide early-stage bone regeneration. Bioact Mater. 2023;25:374–86.
87. Du X, Ronayne S, Lee SS, Hendry J, Hoxworth D, Bock R, et al. 3D-printed PEEK/silicon nitride scaffolds with a triply periodic minimal surface structure for spinal fusion implants. ACS Appl Bio Mater. 2023;6:3319–29.